The pyruvate dehydrogenase complex regulates mitophagic selectivity independently of its catalytic activity

Panagiota Kolitsida[1], Vladimir Nolic[1], Jianwen Zhou[2], Natalie M. Niemi[3], Jörn Dengjel[2] and Hagai Abeliovich[1]

1 Dept. of Biochemistry, Food Science and Nutrition, Hebrew University of Jerusalem, Rehovot, Israel

2 Department of Biology, University of Fribourg, Chemin du Musée 10, 1700 Fribourg, Switzerland

3 Department of Biochemistry and Molecular Biophysics, Washington University, St. Louis, MO

Address correspondence to: Dr. Hagai Abeliovich, Dept. of Biochemistry and Food Science, Hebrew University of Jerusalem, Rehovot, Israel 76100, Tel: 972-8-9489060; Fax: 972-8-9476189; E-mail: hagai.abeliovich@mail.huji.ac.il

Summary

The mitophagic degradation of mitochondrial matrix proteins is selective, reflecting a pre-engulfment sorting step. This selectivity is regulated through phosphorylation of mitochondrial matrix proteins by the matrix kinases Pkp1 and Pkp2, which in turn appear to be regulated by the phosphatase Aup1/Ptc6. However, these proteins also regulate the phosphorylation and catalytic activity of the yeast pyruvate dehydrogenase complex. To understand the relationship between these two functions, we tested the effect of deleting *PDA1* on mitophagic selectivity. We report that *pda1Δ* cells show a mitophagy selectivity phenotype nearly identical to that of the *pkp1Δ pkp2Δ* double mutant. However, this is not due to a role for pyruvate dehydrogenase enzymatic activity in regulating mitophagy. Rather, our data suggest a novel mechanism wherein the pyruvate dehydrogenase complex directly regulates its cognate kinases and phosphatases, independent of its catalytic activity, to determine the phosphorylation state of mitochondrial matrix proteins in response to metabolic cues.

Keywords: mitophagy, protein phosphorylation, pyruvate dehydrogenase complex, mitophagic selectivity, Aup1, Pkp1, Pkp2

Introduction

Mitochondrial autophagy, or mitophagy, is a quality control mechanism that culls defective mitochondria in an effort to prevent cellular damage and dysfunction. Indeed, defects in mitophagic mechanisms have been shown to underlie human pathologies that can be traced to mitochondrial dysfunction. These include Parkinson's disease, Alzheimer's disease and type II diabetes (Vafai and Mootha, 2012; Ploumi *et al.*, 2017; Metaxakis *et al.*, 2018). Known mitophagic mechanisms all involve a receptor protein which interacts with mitochondria on the one hand, and engages the autophagic machinery via LC3/Atg8 proteins and ancillary factors in response to specific cues, on the other hand (Abeliovich and Dengjel, 2016). In mammalian cells, known mitophagy receptors include outer mitochondrial membrane (OMM) cardiolipin, NIX, BNIP3, NDP52, optineurin, prohibitin 2 , TAX1BP1, FUNDC1 and Bcl2-L-13 (Schweers *et al.*, 2007; Bellot *et al.*, 2009; Novak *et al.*, 2010; Liu *et al.*, 2012; Lazarou *et al.*, 2015; Murakawa *et al.*, 2015; Wei *et al.*, 2017), all of which function under different induction conditions and in different cell types. In budding yeast cells, a single OMM protein, Atg32, functions as the only known mitophagy receptor (Kanki *et al.*, 2009; Okamoto *et al.*, 2009). Current thinking envisions the selective activation of a mitophagy receptor on specific mitochondria, which leads to specific engulfment and degradation of those mitochondria. Thus, it is surprising that mitophagic processes, from yeast to man, exhibit protein level selectivity. We previously demonstrated, using SILAC-based proteomics and additional analyses, that different mitochondrial matrix proteins exhibit different mitophagic rates in yeast, and that this phenomenon correlates with physical segregation of the different proteins within the mitochondrial network (Abeliovich *et al.*, 2013). Similar observations were reported in human cells (Hämäläinen *et al.*, 2013; Burman *et al.*, 2017) and in drosophila (Vincow *et al.*, 2013, 2019). More recently, we found that protein phosphorylation in the mitochondrial matrix plays a role in determining intra-mitochondrial mitophagic selectivity. Briefly, we discovered that mitophagic trafficking of the phosphorylated reporter protein Mdh1-GFP depends on its phosphorylation status, and that phosphorylation of the relevant residues requires the function of the mitochondrial matrix kinases Pkp1 and Pkp2, acting under the regulation of the Aup1/Ptc6 phosphatase, which had previously been implicated in mitophagy (Tal *et al.*, 2007; Kolitsida *et al.*, 2019).

Pkp1, Pkp2 and Aup1 have also been shown to regulate the phosphorylation of Pda1, the yeast E1α subunit of the mitochondrial pyruvate dehydrogenase complex (PDC) (Krause-Buchholz *et al.*, 2006; Gey *et al.*, 2008; Guo *et al.*, 2017a). One simple explanation for the data would be that the pyruvate dehydrogenase reaction, which generates acetyl-coA from pyruvate in the mitochondrial matrix, is required for mitophagy or for mitophagic selectivity. However, several problems arise with this hypothesis. For example, in the regulation of pyruvate dehydrogenase activity, Pkp1 and Pkp2 function antagonistically relative to Aup1: they are required for phosphorylation of S313 on Pda1, which inactivates enzymatic activity, while Aup1 mediates dephosphorylation of this residue and activation of the enzyme (Guo *et al.*, 2017a). In contrast, in the regulation of Mdh1-GFP mitophagic trafficking, Pkp2 and Pkp1 function together with Aup1: both the kinases and the phosphatase are required for efficient mitophagy of several reporters, with the kinases functioning downstream of Aup1, as Pkp2 overexpression suppresses the *aup1Δ* phenotype (Kolitsida *et al.*, 2019).

To clarify and reconcile the relationship between the functions of Pkp1, Pkp2, and Aup1 in mitophagy versus their function in Pda1 regulation, we have now examined the potential role of the PDC in generating mitophagic selectivity. Surprisingly, the results of this investigation define a novel signaling cascade that is regulated by the PDC, but is uncoupled from its known enzymatic activity.

Results

Deletion of *PDA1* has a marked effect on mitophagic selectivity, which is uncoupled from pyruvate dehydrogenase activity

Since Aup1, Pkp1 and Pkp2 have been identified as pyruvate kinase phosphatases and kinases (Krause-Buchholz *et al.*, 2006; Gey *et al.*, 2008; González *et al.*, 2013; Guo *et al.*, 2017a), we wanted to understand the relationship between their role in regulating mitophagic selectivity, and their role in regulating pyruvate dehydrogenase activity. Surprisingly, we found that deletion of the *PDA1* gene, which encodes the E1α subunit of the pyruvate dehydrogenase complex (PDC) has a major negative impact on the mitophagic trafficking of 5 different mitochondrial matrix proteins (Figure 1A, B). In contrast, the *pda1Δ* mutation had no effect on the mitophagic trafficking of an artificial mitophagy reporter, mtDHFR-GFP

(Figure 1C, D), as previously reported for the *pkp1Δ pkp2Δ* double mutant (Kolitsida *et al.*, 2019).

The most straightforward explanation for this result would be that the pyruvate dehydrogenase reaction itself, i.e. the formation of acetyl-CoA from pyruvate with concomitant reduction of NAD^+, is required for efficient mitophagy. However, deletion of the mitochondrial pyruvate carrier subunit *MPC1* had no effect on mitophagic trafficking (Figure 2A, B), even though this mutation prevents entry of pyruvate into mitochondria (Herzig *et al.*, 2012). We also tested whether the phosphorylation status of Pda1 at position Ser313 (the residue regulated by Pkp1/2 and Aup1; (Gey *et al.*, 2008; Guo *et al.*, 2017a)) directly determines mitophagic targeting. To this end, we determined whether deletion of *AUP1* can affect mitophagic trafficking in cells where the only copy of *PDA1* encodes a serine to alanine mutation at position 313. As shown in Figure 2C and 2D, the $Pda1^{S313A}$ mutant can weakly complement deletion of the WT protein for mitophagic trafficking of the Mdh1-GFP reporter. However, this residual mitophagic trafficking is completely lost in cells which also lack Aup1, indicating that Aup1 regulates mitophagic trafficking of Mdh1 independently of the phosphorylation state of serine 313 on Pda1. Finally, we tested whether catalytically inactive point mutations in the E1 and E2 subunits affect the mitophagic trafficking of the Mdh1-GFP reporter. For the E1α subunit Pda1, we chose the R322C mutation, which was previously shown to abrogate catalytic activity (Drakulic *et al.*, 2018). As shown in Figure 2E and 2F, this point mutation caused a significant decrease in mitophagic trafficking of Mdh1-GFP, but still allowed a reproducible signal of free GFP under mitophagy inducing conditions, which was significantly higher than that observed in the deletion. More strikingly, when we introduced the un-lipoylatable K75R mutation in the E2 subunit Lat1 (Lawson *et al.*, 1991; Gey *et al.*, 2014), expression of the catalytically inactive mutant subunit led to a clear increase in mitophagic trafficking of Mdh1-GFP, completely opposite from the result expected if the *lat1Δ* phenotype was the result of a block in PDC catalytic activity (Fig. 2G, H). Collectively, these results indicate that the effects of the *pda1Δ* and *lat1Δ* mutations on mitophagic trafficking are not due to the loss of PDC enzymatic activity, nor the phosphorylation status of Serine 313.

Pda1 affects phosphorylation of Mdh1-GFP through the regulation of Pkp1 and Pkp2

The extent of the decrease in mitophagic trafficking of mitochondrial matrix GFP chimeras, which we observe in *pda1Δ* cells (Figure 1A), is very similar to the phenotype which we had previously reported for the *pkp1Δ pkp2Δ* double mutant (Kolitsida *et al.*, 2019). Those previous studies showed that Mdh1-GFP is strongly hypo-phosphorylated in *pkp1Δ pkp2Δ* double mutants (Kolitsida *et al.*, 2019). If the effect of the *pda1Δ* mutation reflects a reciprocal regulation of Aup1, Pkp1 and Pkp2 by the PDC, we would expect that loss of Pda1 would similarly affect the phosphorylation of Mdh1-GFP. Indeed, we find that Mdh1-GFP phosphorylation is strongly attenuated in *pda1Δ* cells, and that this phenotype can be complemented by expressing Pda1 from a plasmid (Figure 3A, B). It was previously shown that Aup1 and Pkp1 stably interact with the PDC (Krause-Buchholz *et al.*, 2006; Breitkreutz *et al.*, 2010; Guo *et al.*, 2017a). It is therefore conceivable that these interactions allosterically regulate the activities of Aup1, Pkp1 and Pkp2. To determine whether the PDC might function upstream of the kinases in regulating mitophagic trafficking of Mdh1-GFP, we first tested if overexpression of Pkp1, Pkp2 or both kinases together, might rescue the mitophagy defect observed in *pda1Δ* cells. As shown in Figure 3C and 3D, co-overexpression of Pkp1 together with Pkp2, but not each kinase separately, causes a near complete rescue of the *pda1Δ* mitophagy phenotype. Finally, co-overexpression of Pkp1 and Pkp2 also increases the phosphorylation of Mdh1-GFP in *pda1Δ* mutants, as would be expected if Pda1 was modulating Pkp1/2 activity towards downstream targets (Figure 4A, 4B), and supporting our finding that it is not the PDC catalytic activity which is affecting the mitophagy of Mdh1-GFP. We were also able to demonstrate a clear PDC-independent physiological function for Pkp1 and Pkp2: While *pda1Δ* cells show a marked reduction in the percentage of colony forming cells following a prolonged incubation in respiratory medium, co-overexpression of Pkp1 and Pkp2 fully suppressed this phenotype (Figure 4C). This result demonstrates that the two kinases have a physiological function other than the regulation of PDC catalytic activity, and at the same time the epistatic relationship indicates, like our other results, that the PDC seems to act as an upstream regulatory element in these novel signaling pathways, independent of its catalytic activity.

If Pda1 regulates Mdh1-GFP phosphorylation via regulation of the activities of Pkp1 and Pkp2, co-deletion of the opposing phosphatase should partially reverse this defect, as any residual phosphorylation activity would now be amplified by the loss of the opposing phosphatase activity. Since our previous work demonstrated that Aup1/Ptc6 cannot be

opposing Pkp1/Pkp2 in this function as 1) deletion of *AUP1* leads to a phenotype that is similar to the phenotypes of *PKP1Δ* and *PKP2Δ*, and 2) Aup1/Ptc6 functions upstream of Pkp2 in regulating Mdh1-GFP phosphorylation and mitophagic trafficking (Kolitsida *et al.*, 2019), we tested the effects of deleting the mitochondrial phosphatases *PTC5* and *PTC7* (Guo *et al.*, 2017a, 2017b), on Mdh1-GFP mitophagic trafficking, in the absence of Pda1. As shown in Figure 4D and 4E, deletion of *PTC5*, and to a much lesser extent deletion of *PTC7*, both led to some generation of free GFP in *pda1Δ* cells, while the phenotype of the combined *ptc5 pdc7* double deletion seems identical to the *ptc5Δ* phenotype. This result further supports the hypothesis that the PDC regulates the phosphorylation state of Mdh1-GFP, and identifies Ptc5 as the main phosphatase which antagonizes the function of Pkp1 and Pkp2 in regulating mitophagic trafficking of Mdh1-GFP.

Deletion of *PDA1* affects protein phosphorylation in the mitochondrial matrix.

Our experiments demonstrate a previously undescribed regulation of mitochondrial protein phosphorylation by the PDC. To determine whether loss of Pda1 can affect the phosphorylation state of additional mitochondrial matrix proteins, we carried out an unbiased phosphoproteomic screen to compare the phosphorylation state of mitochondrial proteins in the presence and absence of Pda1 under our working conditions. To this end, WT (heavy) versus *pda1Δ* (light) cells were differentially labelled with heavy and light isotope-substituted arginine and lysine. The cultures were collected on day 2 of an incubation in synthetic lactate medium (SL), the harvested cells were mixed in equal amounts, and mitochondria were enriched by differential centrifugation. As shown in Figure 5, we were able to identify 19 peptides derived from 8 mitochondrial matrix proteins, whose phosphorylation state was significantly and reproducibly affected by the deletion of *PDA1*. Interestingly, the list includes 3 mitochondrial tRNA ligases, the inner membrane ATP translocase, acyl carnitine transferase, a subunit of the mitochondrial H^+-ATPase, and a component of the electron transport chain. These results further indicate that PDC-mediated regulation of protein phosphorylation in the mitochondrial matrix is not limited to the Mdh1.

Discussion

In this study, we have identified novel regulatory interactions between the pyruvate dehydrogenase complex and its attendant kinases and phosphatase. While previous studies, from the 1960's to the present, have focused on the fact that PDKs regulate pyruvate dehydrogenase activity (Linn *et al.*, 1969; Gey *et al.*, 2008; Guo *et al.*, 2017a; Cardoso *et al.*, 2020), our data now demonstrate that the PDKs have additional substrates, and that their activity towards these non-PDC substrates can be reciprocally regulated by the PDC. This regulation may be mediated via allosteric interactions, as it was previously shown that Pkp1 and Pkp2 function as a heterodimer (Gey *et al.*, 2008; Breitkreutz *et al.*, 2010; Walter *et al.*, 2022) and both Aup1 and Pkp1 stably interact with the PDC (Krause-Buchholz *et al.*, 2006; Guo *et al.*, 2017a). Hundreds of mitochondrial matrix proteins have been documented to undergo phosphorylation (Reinders *et al.*, 2007; Kruse and Højlund, 2017; Renvoisé *et al.*, 2017). However, the nature of the signaling cascades involved and their regulation has remained obscure. Our discovery that Pkp1 and Pkp2 can function to phosphorylate a mitochondrial matrix protein other than Pda1 opens up the possibility that at least some of the documented phosphorylation events in the mitochondrial matrix are due to this novel regulatory axis. In support of this, we found by MS analysis that at least 8 additional mitochondrial matrix proteins show differential phosphorylation in response to deletion of Pda1 under our working conditions (Figure 5). We suggest that some of this regulation can be ascribed to an allosteric effect of the PDC on Aup1/Ptc6. As Aup1 has been shown to interact with the PDC (Guo *et al.*, 2017a), its phosphatase activity could be influenced by this stable physical interaction. Interestingly, the effects of *PDA1* deletion on matrix protein phosphorylation are diverse, with some sites hypophosphorylated and others hyperphosphorylated in the mutant, relative to WT (Fig. 5). In some cases, several peptides within the same protein (Yat1, Vas1) show opposite effects. This may reflect the confounding effects of parallel regulation of Aup1 on the one hand, and Pkp1/Pkp2 on the other hand. Alternatively, this may indicate that the regulation is not a simple on/off switch but rather a change of specificity of the kinases, bringing up the possibility that interaction of Pkp1 and Aup1 with the PDC regulates substrate specificity, and not simply the activity of the kinases.

We propose, based on these results, that the PDC can function as a signaling hub which regulates protein phosphorylation in the mitochondrial matrix in response to metabolic cues (see model in Figure 6). We hypothesize that allosteric transitions in the PDC, induced

by ligand or substrate binding, will affect the structure of the complex, leading to changes in the activity of its associated kinases and phosphatase(s). The entire system, including the redundancy of the pyruvate dehydrogenase kinases (there are 4 PDKs in mammals) and the attendant phosphatase, seems to be highly conserved. Strikingly, the region around the yeast Mdh1 phosphorylation site at Thr199 (IGGHSGITIIPPLISQ), which we previously showed to be crucial for mitophagic trafficking, is also highly conserved in human MDH2 (IGGHAGKTIIPLISQ) and the homologous Thr204 in the human protein was also reported to be phosphorylated (Kettenbach *et al.,* 2011). Therefore, it is likely that these reciprocal interactions are also conserved. Indeed, elegant biochemical studies from the Roche lab demonstrated that the activation of human PDK2 by NADH and acetyl coA was due to bound E2 becoming acetylated in the partial reverse reaction, demonstrating the existence of this exact type of allosteric coupling in human PDKs (Baker *et al.*, 2000). Also in line with this argument, it was recently reported that the overexpression of *PDK4* enhances mitophagy in mammalian cells (Park *et al.*, 2015). Another recent study found that branched-chain amino acids allosterically modulate PDC activity (Li *et al.*, 2017), supporting the possibility that metabolically-induced conformational changes in the PDC regulate matrix protein phosphorylation through protein-protein interactions with PDC-associated kinase and phosphatases.

The concept of large signaling complexes that integrate metabolic cues to regulate cellular activity has been the focus of intense study recently. TORC1 and TORC2 are example of such mega-complexes, which integrate nitrogen, amino acid and carbohydrate metabolism with hormone signaling, to generate readouts which regulate cellular responses to changes in the environment (Eltschinger and Loewith, 2016; Nicastro *et al.*, 2017; Szwed *et al.*, 2021). We hypothesize that the PDC could serve a similar function within mitochondria, by regulating matrix protein phosphorylation in response to changes in metabolite levels. Further work will now be required to test specific aspects of this hypothesis.

Methods

Yeast strains, plasmids and growth conditions

Yeast strains used in this study are listed in Supplementary Table I. Deletion mutants and epitope-tagged strains were generated by the cassette integration method (Longtine *et al.*, 1998). Strain HAY75 (MATα *leu2-3,112 ura3-52 his3-Δ200 trp1-Δ901 lys2-801 suc2-Δ9*) was used as the WT genetic background in this study..

All knockout strains were verified by PCR. Oligonucleotides used in this study are detailed in Supplementary Table III, and plasmids are detailed in Supplementary Table II.

Yeast were grown in synthetic dextrose medium (0.67% yeast nitrogen base w/o amino acids (Difco), 2% glucose, auxotrophic requirements and vitamins as required) or in SL medium (0.67% yeast nitrogen base w/o amino acids (Difco), 2% lactate pH 6, 0.1% glucose, auxotrophic requirements and vitamins as required). All culture growth and manipulation were at 26 ^{0}C. Yeast transformation was according to Gietz and Woods (Gietz and Woods, 2002).

For nitrogen starvation experiments, cells were grown to mid-log phase (OD_{600} of 0.4-0.6) in synthetic dextrose medium (SD), washed with distilled water, and resuspended in nitrogen starvation medium (0.17% yeast nitrogen base lacking amino acids and ammonium sulfate (Difco), 2% glucose) for the times indicated in individual experiments. Overexpression studies with *CUP1* promoter-based vectors were carried out by supplementing the medium with 5 μM $CuSO_4$, for both control (empty vector) and overexpressing cells.

Chemicals and antisera

Chemicals were purchased from Sigma-Aldrich (Rehovot, Israel) unless otherwise stated. Custom oligonucleotides were from Hylabs (Rehovot, Israel). Anti-GFP antiserum was from Santa-Cruz (Dallas, TX). Horseradish peroxidase-conjugated goat anti-rabbit antibodies were from MP Biomedicals (Santa Ana, CA). Anti-phosphoserine/threonine antibodies were from ECM Biosciences (catalog # PM3801).

Preparation of whole-cell extracts for western blot analysis

Cells (10 OD_{600} units) were treated with 10% cold trichloroacetic acid (TCA) and washed three times with cold acetone. The dry cell pellet was then resuspended in 100 μl cracking

buffer (50 mM Tris pH 6.8, 6 M urea, 1 mM EDTA, 1% SDS) and vortexed in a Heidolf Multi Reax microtube mixer at maximum speed with an equal volume of acid-washed glass beads (425-600µm diameter), for a total of 30 min. Lysates were clarified by centrifugation at 17,000 xg for 5 min and total protein was quantified in the supernatant using the BCA protein assay (Thermo Scientific, Rockford, IL). SDS loading buffer (final concentrations of 100 mM Tris pH 6.8, 20% glycerol, 2% SDS, 500 mM β-mercaptoethanol) was added to the lysate and the samples were warmed to 60 °C for 5 min prior to loading on gels. ImageJ software was used for band quantification.

Immunoblotting

SDS-10% polyacrylamide gels were transferred to nitrocellulose membrane by using either a wet or semidry blotting transfer system. Membranes were blocked for 1 h with TPBS (137 mM NaCl, 2.7 mM KCL, 10 mM Na_2HPO_4, 1.8 mM KH_2PO_4, 1 % Tween and 5 % milk powder (BD Difco Skim Milk), followed by incubation with rabbit anti-GFP (1:5000) for 1.5 h, then washed 4x 2 min with TPBS, incubated for 1.5 h with HRP conjugated secondary antibody (1:10000). The membranes were then washed 4x with TPBS, incubated with SuperSignal Chemiluminescence substrate (Thermo Scientific), and exposed to a Molecular Imager ChemiDoc™ XRS imaging system. Where necessary, 2% normal goat serum was added to blocking solutions to reduce background.

Calculation of statistical significance of differences in % free GFP signals from immunoblots

Data (% free GFP) were log-transformed before analysis in order to stabilize variances. A repeated measures ANOVA was performed to compare mutants and proteins simultaneously. Thereafter, mutants were compared for each protein and proteins were compared for each mutant by the Tukey HSD test ($p<0.05$). ANOVA analysis was carried out using JMP 12 software.

Native immunoprecipitation.

Cells (20 OD_{600} units) were washed 3x with 1 ml of cold 10 mM PIPES pH 7, 2 mM PMSF. The cell pellet was washed in three volumes of cold lysis buffer (20 mM HEPES pH 7.4, 50 mM NaCl, 1mM EDTA, 10% glycerol, 0.2 mM Na_3VO_4, 10 mM H_2NaPO_4, 10 mM β-glycerophosphate, 10 mM NaF, 10% phosphate cocktail inhibitors, 1 mM PMSF, proteases

inhibitors (final concentrations: 5 µg/ ml antipain, 1 µg/ml aprotinin, 0.5 µg/ml leupeptin, 0.7 µg/ml pepstatin). The cells were then frozen in liquid nitrogen and stored at -80°C. Extracts were prepared from the frozen pellets using a SPEX Freezer/Mill according to the manufacturer's instruction. The frozen ground yeast powder was thawed at room temperature, and equal amount of lysis buffer plus Triton-X100 was added to a final concentration of 0.5% v/v detergent. Cell debris was removed by centrifugation at 17.000x g for 10 min at 4°C. 20 µl of GFP-Trap bead slurry (Chromotek) was pre-equilibrated in lysis buffer, per the manufacturer's instructions. The cleared lysate was added to the equilibrated beads and incubated for 1 h at 4 °C with constant mixing. The beads were washed five times with 1 ml ice cold wash buffer (20 mM HEPES pH 7.4, 50 mM NaCl, 0.5 mM EDTA, 10% glycerol, 0.5% Triton-X, 0.2 mM $NaOV_3$, 10 mM H_2NaPO_3, 10 mM β-glycerophosphate, 10 mM NaF, resuspended in 50 µl 2x SDS-loading buffer (200 mM Tris pH 6.8, 40% glycerol, 4% SDS, 1 M β-mercaptoethanol) and boiled for 10 min at 95°C. For phosphatase treatment, immunoprecipitated beads were incubated with 40 Units of lambda protein phosphate (New England Biolabs) in a 50 µl reaction. Samples were washed once with wash buffer and resuspended in 50 µl 2 x SDS-loading buffer.

SILAC labeling

To quantify relative phosphorylation on mitochondrial proteins in WT versus *pda1Δ* backgrounds, cell cultures of each strain were grown separately in SL medium supplemented respectively with 0.003% (w/v) $^{13}C_6\,^{15}N_2$ L-lysine (Lys8; Cat. Number 211604102, Silantes, Munich) and 0.001% (w/v) $^{13}C_6{}^{15}N_4$ L-arginine (Arg10; Cat. Number 201603902, Silantes, Munich) or with identical concentrations of unlabeled lysine and arginine, in addition to the standard auxotrophy supplementation. At the indicated time point, 50 OD_{600} units of cells from each labeling regime were combined, washed with cold lysis buffer, and cells were frozen in liquid nitrogen. To lyse the cells, the frozen suspensions were processed in a SPEX Freezer/Mill according to the manufacturers' instructions. The frozen ground powder was thawed and clarified by centrifuging for 10 min at 500 xg. The clarified lysates were then further centrifuged for 10 min at 13,000 xg, the supernatant was discarded and the pellet was precipitated with 10% ice cold TCA and washed 3x with cold acetone.

MS analysis

Mass spectrometric measurements were performed on a Q Exactive HF-X mass spectrometer coupled to an EasyLC 1200 (Thermo Fisher Scientific, Bremen, Germany). Prior to analysis phosphopeptides were enriched on an Automated Liquid Handling Platform (AssayMap Bravo, Agilent) using Fe (III)-NTA cartridges (5 μL) essentially as described previously (PMID: 28107008). The MS raw data files were analysed by the MaxQuant software (Cox and Mann, 2008) version 1.4.1.2, using a Uniprot *Saccharomyces cerevisiae* database from March 2016 containing common contaminants such as keratins and enzymes used for in-gel digestion.

Statistical analysis

Phosphosite SILAC ratios were normalized to respective protein changes to discriminate regulated sites from regulated proteins. Measurements of three biological replicates (Pearson correlation of 0.64- 071) comparing WT to *pda1Δ* cells were averaged and log2 transformed. To determine sites that changed significantly between genotypes we calculated an outlier significance score on the merged log2-tarnsformed phosphosite ratios according to (Cox and Mann, 2008) (significance A, $p<0.05$, BH corrected).

Site directed mutagenesis

Site directed mutagenesis protocol was carried out according to the Stratagene QuikChange system. *Pfu* DNA Polymerase (Fermentas) was used with a thermocycling protocol followed by removal of the parental strands with *DpnI* digestion. Thermocycling conditions were as follows: Initial denaturation at 95°C for 2 min, then (steps 2-4), 30 sec at 95 ^{o}C, 60 sec at 55 ^{o}C, and 12 min at 68 ^{o}C. Steps 2-4 repeated for 18 cycles. PCR products were treated with DpnI (fermentas) for 1 hr at 37 ^{o}C, and precipitated using with 70% ethanol. DNA pellets were then dried and resuspended with 20 µl TE buffer pH 8. All mutagenesis products were transformed into *E. coli* DH5α and mutations were verified by sequencing. The oligonucleotide primers used to create site-directed MDH1-GFP variants and combined variants are listed in Supplementary Table III.

Acknowledgements

We wish to thank J.C. Martinou and Maya Schuldiner for discussions. This work was funded by ISF grant 422/12 (to HA), ISF grant 445/17 (to HA), GIF grant I-111-412.7-2014 (to HA and JD), the University and Canton of Fribourg and the Swiss National Science Foundation (J.D.).

Author contributions

P.K. planned experiments, carried out experiments, generated figures, and wrote the manuscript. V. N. carried out experiments. J.Z. carried out MS analyses. N.N. planned experiments and wrote the manuscript. J.D. carried out MS analyses, planned experiments, generated figures, and wrote the manuscript. H.A. Planned experiments, generated figures, and wrote the manuscript.

Bibliography

Abeliovich H, Dengjel J (2016) Mitophagy as a stress response in mammalian cells and in respiring S. cerevisiae. *Biochem Soc Trans*, **44:** 541–545

Abeliovich H, Zarei M, Rigbolt KT, Youle RJ, Dengjel J (2013) Involvement of mitochondrial dynamics in the segregation of mitochondrial matrix proteins during stationary phase mitophagy. *Nat Commun*, **4:** 2789

Baker JC, Yan X, Peng T, Kasten S, Roche TE (2000) Marked differences between two isoforms of human pyruvate dehydrogenase kinase. *J Biol Chem*, **275:** 15773–15781

Bellot G, Garcia-Medina R, Gounon P, Chiche J, Roux D, Pouysségur J, Mazure NM (2009) Hypoxia-induced autophagy is mediated through hypoxia-inducible factor induction of BNIP3 and BNIP3L via their BH3 domains. *Mol Cell Biol*, **29:** 2570–2581

Breitkreutz A, Choi H, Sharom JR, Boucher L, Neduva V, Larsen B, Lin ZY, Breitkreutz BJ, Stark C, Liu G, Ahn J, Dewar-Darch D, Reguly T, Tang X, Almeida R, Qin ZS, Pawson T, Gingras AC, Nesvizhskii AI, Tyers M (2010) A global protein kinase and phosphatase interaction network in yeast. *Science*, **328:** 1043–1046

Burman JL, Pickles S, Wang C, Sekine S, Vargas JNS, Zhang Z, Youle AM, Nezich CL, Wu X, Hammer JA, Youle RJ (2017) Mitochondrial fission facilitates the selective mitophagy of protein aggregates. *J Cell Biol*, **216:** 3231–3247

Cardoso AC, Lam NT, Savla JJ, Nakada Y, Pereira AHM, Elnwasany A, Menendez-Montes I, Ensley EL, Petric UB, Sharma G, Sherry AD, Malloy CR, Khemtong C, Kinter MT, Tan WLW, Anene-Nzelu CG, Foo RS, Nguyen NUN, Li S, Ahmed MS, Elhelaly WM, Abdisalaam S, Asaithamby A, Xing C, Kanchwala M, Vale G, Eckert KM, Mitsche MA, McDonald JG, Hill JA, Huang L, Shaul PW, Szweda LI, Sadek HA (2020) Mitochondrial Substrate Utilization Regulates Cardiomyocyte Cell Cycle Progression. *Nat Metab*, **2:** 167–178

Cox J, Mann M (2008) MaxQuant enables high peptide identification rates, individualized p.p.b.-range mass accuracies and proteome-wide protein quantification. *Nat Biotechnol*, **26:** 1367–1372

Drakulic S, Rai J, Petersen SV, Golas MM, Sander B (2018) Folding and assembly defects of pyruvate dehydrogenase deficiency-related variants in the E1α subunit of the pyruvate dehydrogenase complex. *Cell Mol Life Sci*, **75:** 3009–3026

Eltschinger S, Loewith R (2016) TOR Complexes and the Maintenance of Cellular Homeostasis. *Trends Cell Biol*, **26:** 148–159

Gey U, Czupalla C, Hoflack B, Krause U, Rödel G (2014) Proteomic analysis reveals a novel function of the kinase Sat4p in Saccharomyces cerevisiae mitochondria. *PLoS One*, **9:** 103956

Gey U, Czupalla C, Hoflack B, Rödel G, Krause-Buchholz U (2008) Yeast pyruvate dehydrogenase complex is regulated by a concerted activity of two kinases and two phosphatases. *J Biol Chem*, **283:** 9759–9767

Gietz RD, Woods RA (2002) Transformation of yeast by lithium acetate/single-stranded carrier DNA/polyethylene glycol method. *Methods Enzymol*, **350:** 87–96

González A, Casado C, Ariño J, Casamayor A (2013) Ptc6 is required for proper rapamycin-induced down-regulation of the genes coding for ribosomal and rRNA processing proteins in S. cerevisiae. *PLoS One*, **8:** e64470

Guo X, Niemi NM, Coon JJ, Pagliarini DJ (2017a) Integrative proteomics and biochemical analyses define Ptc6p as the Saccharomyces cerevisiae pyruvate dehydrogenase phosphatase. *J Biol Chem*, **292:** 11751–11759

Guo X, Niemi NM, Hutchins PD, Condon SGF, Jochem A, Ulbrich A, Higbee AJ, Russell JD, Senes A, Coon JJ, Pagliarini DJ (2017b) Ptc7p Dephosphorylates Select Mitochondrial Proteins to Enhance Metabolic Function. *Cell Rep*, **18:** 307–313

Hämäläinen RH, Manninen T, Koivumäki H, Kislin M, Otonkoski T, Suomalainen A (2013) Tissue- and cell-type-specific manifestations of heteroplasmic mtDNA 3243A>G mutation in human induced pluripotent stem cell-derived disease model. *Proc Natl Acad Sci U S A*, **110:** E3622–30

Herzig S, Raemy E, Montessuit S, Veuthey JL, Zamboni N, Westermann B, Kunji ER, Martinou JC (2012) Identification and functional expression of the mitochondrial pyruvate carrier. *Science*, **337:** 93–96

Kanki T, Wang K, Cao Y, Baba M, Klionsky DJ (2009) Atg32 is a mitochondrial protein that confers selectivity during mitophagy. *Dev Cell*, **17:** 98–109

Kettenbach AN, Schweppe DK, Faherty BK, Pechenick D, Pletnev AA, Gerber SA (2011) Quantitative phosphoproteomics identifies substrates and functional modules of Aurora and Polo-like kinase activities in mitotic cells. *Sci Signal*, **4:** rs5

Kolitsida P, Zhou J, Rackiewicz M, Nolic V, Dengjel J, Abeliovich H (2019) Phosphorylation of mitochondrial matrix proteins regulates their selective mitophagic degradation. *Proc Natl Acad Sci U S A*, **116:** 20517–20527

Krause-Buchholz U, Gey U, Wünschmann J, Becker S, Rödel G (2006) YIL042c and YOR090c encode the kinase and phosphatase of the Saccharomyces cerevisiae pyruvate dehydrogenase complex. *FEBS Lett*, **580:** 2553–2560

Kruse R, Højlund K (2017) Mitochondrial phosphoproteomics of mammalian tissues. *Mitochondrion*, **33:** 45–57

Lawson JE, Niu XD, Reed LJ (1991) Functional analysis of the domains of dihydrolipoamide acetyltransferase from Saccharomyces cerevisiae. *Biochemistry*, **30:** 11249–11254

Lazarou M, Sliter DA, Kane LA, Sarraf SA, Wang C, Burman JL, Sideris DP, Fogel AI, Youle RJ (2015) The ubiquitin kinase PINK1 recruits autophagy receptors to induce mitophagy. *Nature*, **524:** 309–314

Li T, Zhang Z, Kolwicz SC, Abell L, Roe ND, Kim M, Zhou B, Cao Y, Ritterhoff J, Gu H, Raftery D, Sun H, Tian R (2017) Defective Branched-Chain Amino Acid Catabolism Disrupts Glucose Metabolism and Sensitizes the Heart to Ischemia-Reperfusion Injury. *Cell Metab*, **25:** 374–385

Linn TC, Pettit FH, Reed LJ (1969) Alpha-keto acid dehydrogenase complexes. X. Regulation of the activity of the pyruvate dehydrogenase complex from beef kidney mitochondria by phosphorylation and dephosphorylation. *Proc Natl Acad Sci U S A*, **62:** 234–241

Liu L, Feng D, Chen G, Chen M, Zheng Q, Song P, Ma Q, Zhu C, Wang R, Qi W, Huang L, Xue P, Li B, Wang X, Jin H, Wang J, Yang F, Liu P, Zhu Y, Sui S, Chen Q (2012) Mitochondrial outer-membrane protein FUNDC1 mediates hypoxia-induced mitophagy in mammalian cells. *Nat Cell Biol*, **14:** 177–185

Longtine MS, McKenzie A, Demarini DJ, Shah NG, Wach A, Brachat A, Philippsen P, Pringle JR (1998) Additional modules for versatile and economical PCR-based gene deletion and modification in Saccharomyces cerevisiae. *Yeast*, **14:** 953–961

Metaxakis A, Ploumi C, Tavernarakis N (2018) Autophagy in Age-Associated Neurodegeneration. *Cells*, **7:**

Murakawa T, Yamaguchi O, Hashimoto A, Hikoso S, Takeda T, Oka T, Yasui H, Ueda H, Akazawa Y, Nakayama H, Taneike M, Misaka T, Omiya S, Shah AM, Yamamoto A, Nishida K, Ohsumi Y, Okamoto K, Sakata Y, Otsu K (2015) Bcl-2-like protein 13 is a mammalian Atg32 homologue that mediates mitophagy and mitochondrial fragmentation. *Nat Commun*, **6:** 7527

Nicastro R, Sardu A, Panchaud N, De Virgilio C (2017) The Architecture of the Rag GTPase Signaling Network. *Biomolecules*, **7:** E48

Novak I, Kirkin V, McEwan DG, Zhang J, Wild P, Rozenknop A, Rogov V, Löhr F, Popovic D, Occhipinti A, Reichert AS, Terzic J, Dötsch V, Ney PA, Dikic I (2010) Nix is a selective autophagy receptor for mitochondrial clearance. *EMBO Rep*, **11:** 45–51

Okamoto K, Kondo-Okamoto N, Ohsumi Y (2009) Mitochondria-anchored receptor Atg32 mediates degradation of mitochondria via selective autophagy. *Dev Cell*, **17:** 87–97

Park S, Choi SG, Yoo SM, Nah J, Jeong E, Kim H, Jung YK (2015) Pyruvate stimulates mitophagy via PINK1 stabilization. *Cell Signal*, **27:** 1824–1830

Ploumi C, Daskalaki I, Tavernarakis N (2017) Mitochondrial biogenesis and clearance: a balancing act. *FEBS J*, **284:** 183–195

Reinders J, Wagner K, Zahedi RP, Stojanovski D, Eyrich B, van der Laan M, Rehling P, Sickmann A, Pfanner N, Meisinger C (2007) Profiling phosphoproteins of yeast mitochondria reveals a role of phosphorylation in assembly of the ATP synthase. *Mol Cell Proteomics*, **6:** 1896–1906

Renvoisé M, Bonhomme L, Davanture M, Zivy M, Lemaire C (2017) Phosphoproteomic Analysis of Isolated Mitochondria in Yeast. *Methods Mol Biol*, **1636:** 283–299

Schweers RL, Zhang J, Randall MS, Loyd MR, Li W, Dorsey FC, Kundu M, Opferman JT, Cleveland JL, Miller JL, Ney PA (2007) NIX is required for programmed mitochondrial clearance during reticulocyte maturation. *Proc Natl Acad Sci U S A*, **104:** 19500–19505

Szwed A, Kim E, Jacinto E (2021) Regulation and metabolic functions of mTORC1 and mTORC2. *Physiol Rev*, **101:** 1371–1426

Tal R, Winter G, Ecker N, Klionsky DJ, Abeliovich H (2007) Aup1p, a yeast mitochondrial protein phosphatase homolog, is required for efficient stationary phase mitophagy and cell survival. *J Biol Chem*, **282:** 5617–5624

Vafai SB, Mootha VK (2012) Mitochondrial disorders as windows into an ancient organelle. *Nature*, **491:** 374–383

Vincow ES, Merrihew G, Thomas RE, Shulman NJ, Beyer RP, MacCoss MJ, Pallanck LJ (2013) The PINK1-Parkin pathway promotes both mitophagy and selective respiratory chain turnover in vivo. *Proc Natl Acad Sci U S A*, **110:** 6400–6405

Vincow ES, Thomas RE, Merrihew GE, Shulman NJ, Bammler TK, MacDonald JW, MacCoss MJ, Pallanck LJ (2019) Autophagy accounts for approximately one-third of mitochondrial protein turnover and is protein selective. *Autophagy*, 1–14

Walter C, Marada A, Meisinger C (2022) Monitoring checkpoints of metabolism and protein biogenesis in mitochondria by Phos-tag technology. *J Proteomics*, **252:** 104430

Wei Y, Chiang WC, Sumpter R, Mishra P, Levine B (2017) Prohibitin 2 Is an Inner Mitochondrial Membrane Mitophagy Receptor. *Cell*, **168:** 224–238.e10

Figure legends

Figure 1. **Loss of *PDA1* affects mitophagic trafficking and selectivity of mitochondrial matrix proteins**. WT and *pda1Δ* cells expressing the indicated GFP-tagged mitochondrial matrix proteins were grown in SL medium as indicated in "Methods". Samples were taken on days 1 and 5, and protein extracts were analyzed by anti-GFP immunoblotting. A. Loss of *PDA1* strongly attenuates mitophagic trafficking of Mdh1-GFP and this can be complemented by expressing Pda1 from a plasmid. B. Loss of *PDA1* strongly attenuates the mitophagic trafficking of endogenous GFP chimeras of five different mitochondrial matrix proteins. C. Loss of *PDA1* does not affect mitophagic trafficking of an artificial mitochondrial GFP fusion protein, mtDHFR-GFP. Deletion of *ATG32* is included as a negative control. D. Quantification of the data from (C). Data are shown from 3 independent biological replicates +/- standard deviation. ϕ denotes empty vector.

Figure 2. **The effects of *PDA1* deletion on mitophagy are not mediated through the pyruvate dehydrogenase reaction, and mitophagic trafficking can be modulated independent of S313 phosphorylation**. A. Loss of *MPC1* has no effect on mitophagic trafficking of Mdh1-GFP. WT, *mpc1Δ* and *pda1Δ* cells expressing Mdh1-GFP were grown in SL medium for the indicated amounts of time and protein extracts were generated. The extracts were analyzed by immunoblotting with α-GFP antibodies. B. Quantification of the data in A. C. Cells expressing the S313A Pda1 point mutant still exhibit an *AUP1*- dependent mitophagic trafficking phenotype despite the absence of phosphoserine 313. Cell handling was as in (A), but only the day 5 samples are shown. D. Quantification of the data in C. E. The catalytically inactive $pda1^{R322C}$ mutant can support partial mitophagic trafficking of Mdh1-GFP. Only day 5 samples are shown for brevity. F. Quantification of the data in E. G. The unlipoylatable $lat1^{K75R}$ mutant shows increased mitophagic trafficking of Mdh1-GFP, relative to WT. Only day 5 samples are shown, for brevity. G. Quantification of the data in F. All quantifications are presented as averages of 3 independent biological replicates with standard deviation depicted as error bars. ϕ denotes empty vector.

Figure 3. **PDC regulates phosphorylation of Mdh1.** A. The *pda1Δ* mutation causes hypophosphorylation of Mdh1-GFP. WT and *pda1Δ* cells expressing Mdh1-GFP were grown in SL medium for the indicated amounts of time and protein extracts were generated and immunoprecipitated with α-GFP antibody. The immunoprecipitates were then probed with α-phosphoamino acid antibody (top panel) and α-GFP antibody (bottom panel). Right panel: day 5 samples were treated overnight with lambda phosphatase or mock treated as described in "Methods" and analyzed by immunoblotting. B. Quantification of the data in (A). The results of 3 independent biological repeats were quantified by normalizing the α-phosphoamino acid signal to the GFP signal, and averaged. C. Co-overexpression of Pkp1 and Pkp2 completely suppresses the mitophagy defect of *pda1Δ* cells. WT and *pda1Δ* cells expressing Mdh1-GFP as well as the indicated plasmids, were grown in SL medium for 5 days and protein extracts were generated. The extracts were analyzed by immunoblotting with α-GFP antibodies. D. Quantification of the data in (C). The results of 3 independent biological repeats were quantified by calculating the % free GFP relative to the total signal (N=3). ϕ denotes empty vector.

Figure 4. **Co-overexpression of Pkp1 and Pkp2 recovers the phosphorylation of Mdh1-GFP in *pda1Δ* cells**. A. WT and *pda1Δ* cells expressing Mdh1-GFP as well as the indicated plasmids were grown in SL medium for the indicated amounts of time and protein extracts were generated and immunoprecipitated with α-GFP antibody. Phosphorylation of Mdh1-GFP was detected using α-phosphoamino acid antibody and total GFP signal in the immunoprecipitate was observed by immunoblotting with α-GFP antibody. ϕ denotes empty vector. B. Quantification of the data in (A). The results of 3 independent biological repeats were quantified by normalizing the α-phosphoamino acid signal to the GFP signal, and averaged. C. Pkp1 and Pkp2 have a physiological function independent of pda1 phosphorylation. Cells were grown to late log phase in SD medium, washed and equal cell numbers were resuspended in SL medium. Cell viability was measured by plating diluted aliquots on rich YPD medium after 5 days of incubation in SL medium. Clearly, co-overexpression of Pkp1 and Pkp2 completely suppresses the defect in *pda1Δ* cells. D. Deletion of PTC5 partially suppresses the *pda1Δ* mitophagy defect. Mdh1-GFP- expressing WT, *pda1Δ,* and *pda1Δ* cells harboring co deletions of *PTC7*, *PTC5* or both, were incubated

in SL medium for 5 days and protein extracts were generated. The extracts were analyzed by immunoblotting with α-GFP antibodies. E. Quantification of 3 independent biological repeats of the experiment shown in D.

Figure 5. **Deletion of *PDA1* has general effects on protein phosphorylation in the mitochondrial matrix**. A. Overview of the methodology. WT cells and *pda1Δ* cells expressing mtRFP were grown for 2 days in SL medium containing heavy lysine+arginine (WT) or regular lysine+arginine (*pda1Δ*). Equivalent amounts of WT and *pda1Δ* cells were combined (see Materials and Methods) and cell extracts were generated by gentle cryomilling. The extract was further centrifuged at 13000 xg and the pellet was analyzed by microscopic examination (100x objective) to verify the enrichment of intact mitochondria relative to total extract (B). DIC images are included to verify the absence of intact cells. C. Quantitative SILAC MS/MS comparison of mitochondrial phosphopeptides identified in WT and *pda1Δ* mutants. Significant hits are annotated by protein. Phosphorylated positions are denoted in superscript.

Figure 6. **Model for regulation of mitochondrial protein phosphorylation by the PDC.** We propose that the known stable physical interactions between Aup1 and Pda1 (ref. 22) and between Pkp1 and Pda1 (ref. 23) can function as an allosteric interface to regulate Aup1, Pkp1 and Pkp2 activity towards other proteins within the mitochondrial matrix. We previously showed that Pkp2 functions downstream of Aup1, and in this study we showed that co-overexpression of Pkp1 and Pkp2 completely overcomes the mitophagy defect in *pda1Δ* cells. It remains to be seen whether physiological PDC ligands can allosterically regulate phosphorylation in the matrix. Since we also showed that Aup1 functions upstream of Pkp2 in regulating mitophagy, and we now demonstrate that the mitophagy-related function of Aup1 is independent of Pda1 phosphorylation, we propose that Pda1- bound Aup1 functions downstream of Pda1 to transduce signals to the kinase(s) in the pathway, although theoretically Aup1 may also affect Pkp2 completely independent from Pda1.

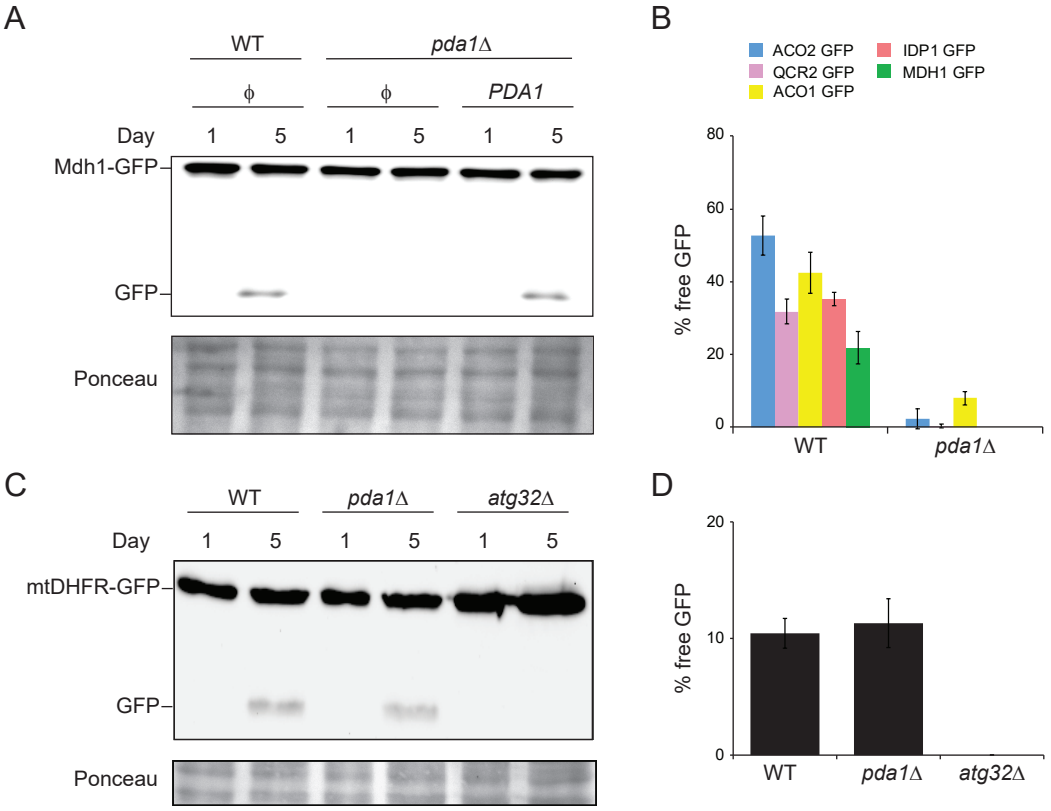
A
WT
pda1Δ
ϕ
ϕ
PDA1
Day
1
5
1
5
1
5
Mdh1-GFP
GFP
Ponceau
B
ACO2 GFP
QCR2 GFP
ACO1 GFP
IDP1 GFP
MDH1 GFP
% free GFP
80
60
40
20
0
WT
pda1Δ
C
WT
pda1Δ
atg32Δ
Day
1
5
1
5
1
5
mtDHFR-GFP
GFP
Ponceau
D
% free GFP
20
10
0
WT
pda1Δ
atg32Δ

Figure 1

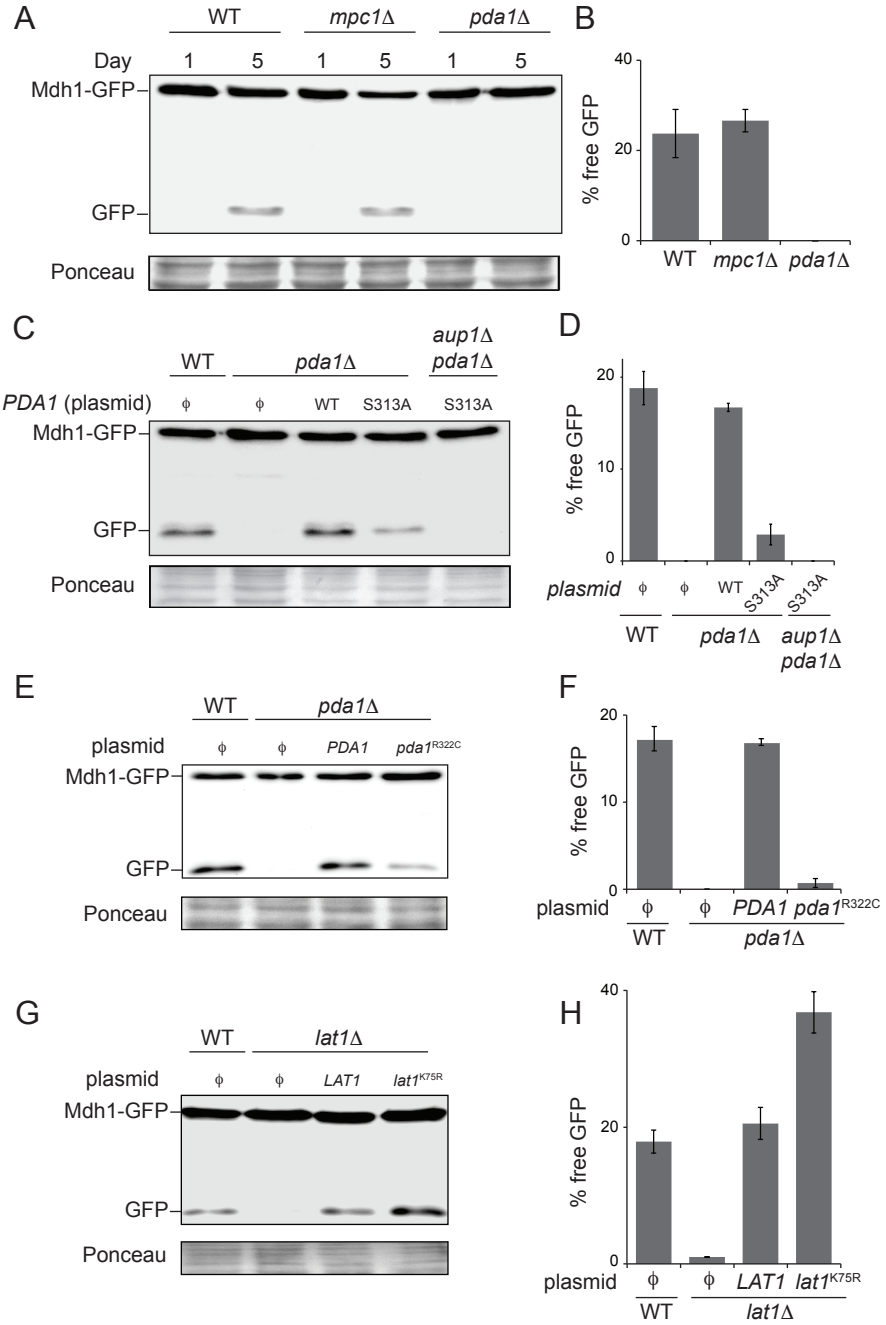
A
WT
mpc1Δ
pda1Δ
Day
1
5
1
5
1
5
Mdh1-GFP
GFP
Ponceau
B
% free GFP
40
20
0
WT
mpc1Δ
pda1Δ
C
WT
pda1Δ
aup1Δ pda1Δ
PDA1 (plasmid)
ϕ
ϕ
WT
S313A
S313A
Mdh1-GFP
GFP
Ponceau
D
% free GFP
20
10
0
plasmid
ϕ
ϕ
WT
S313A
S313A
WT
pda1Δ
aup1Δ pda1Δ
E
WT
pda1Δ
plasmid
ϕ
ϕ
PDA1
pda1R322C
Mdh1-GFP
GFP
Ponceau
F
% free GFP
20
10
0
plasmid
ϕ
ϕ
PDA1
pda1R322C
WT
pda1Δ
G
WT
lat1Δ
plasmid
ϕ
ϕ
LAT1
lat1K75R
Mdh1-GFP
GFP
Ponceau
H
% free GFP
40
20
0
plasmid
ϕ
ϕ
LAT1
lat1K75R
WT
lat1Δ

Figure 2

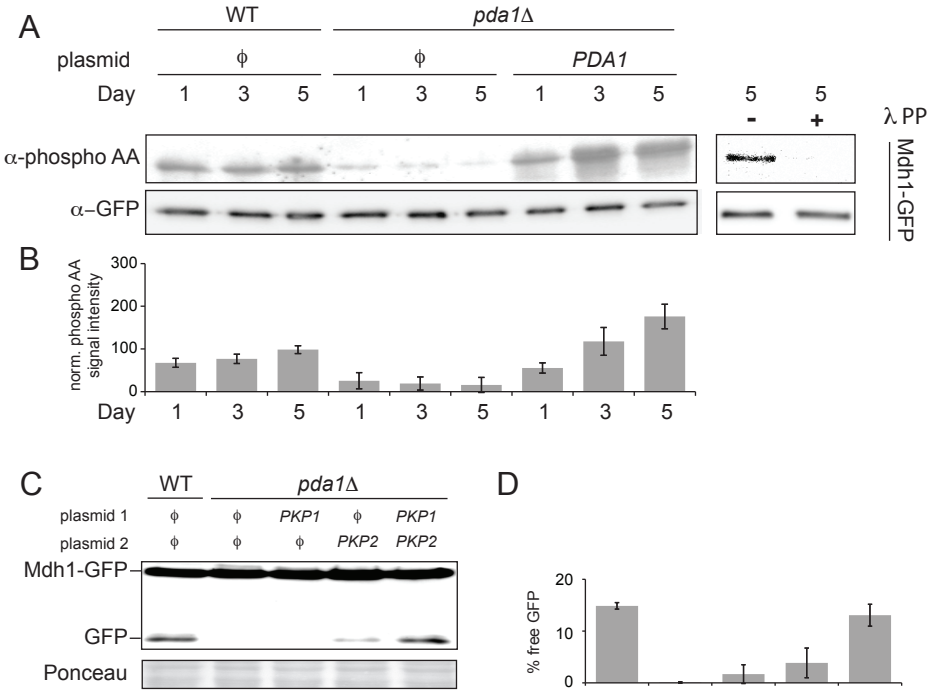
A
WT
pda1Δ
plasmid
ϕ
ϕ
PDA1
Day
1 3 5 1 3 5 1 3 5
5 5
- +
λ PP
α-phospho AA
α–GFP
Mdh1-GFP
B
norm. phospho AA signal intensity
300
200
100
0
Day
1 3 5 1 3 5 1 3 5
C
WT
pda1Δ
plasmid 1
ϕ ϕ PKP1 ϕ PKP1
plasmid 2
ϕ ϕ ϕ PKP2 PKP2
Mdh1-GFP
GFP
Ponceau
D
% free GFP
20
10
0

Figure 3

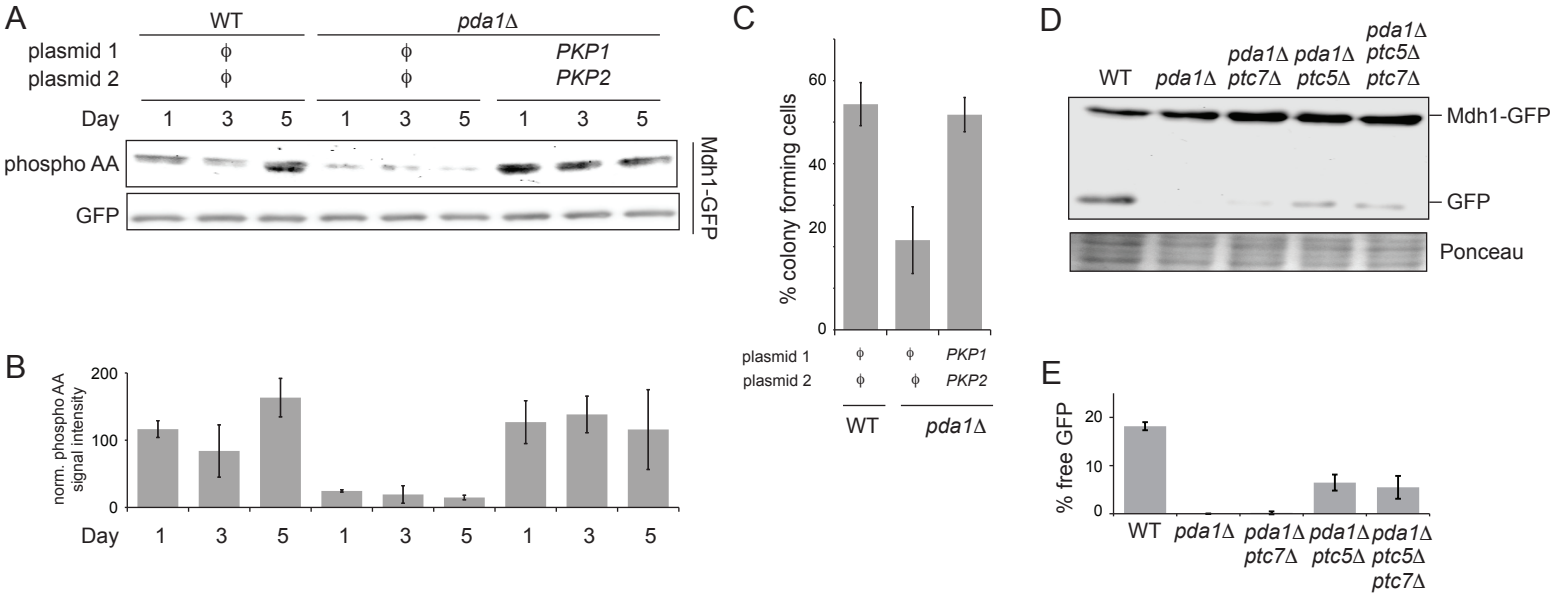
A
WT
pda1Δ
plasmid 1
plasmid 2
ϕ
PKP1
PKP2
Day
1 3 5 1 3 5 1 3 5
phospho AA
GFP
Mdh1-GFP
B
norm. phospho AA signal intensity
200
100
0
Day
1 3 5 1 3 5 1 3 5
C
% colony forming cells
60
40
20
0
plasmid 1
plasmid 2
ϕ ϕ PKP1
ϕ ϕ PKP2
WT
pda1Δ
D
WT
pda1Δ
pda1Δ ptc7Δ
pda1Δ ptc5Δ
pda1Δ ptc5Δ ptc7Δ
Mdh1-GFP
GFP
Ponceau
E
% free GFP
20
10
0
WT
pda1Δ
pda1Δ ptc7Δ
pda1Δ ptc5Δ
pda1Δ ptc5Δ ptc7Δ

Figure 4

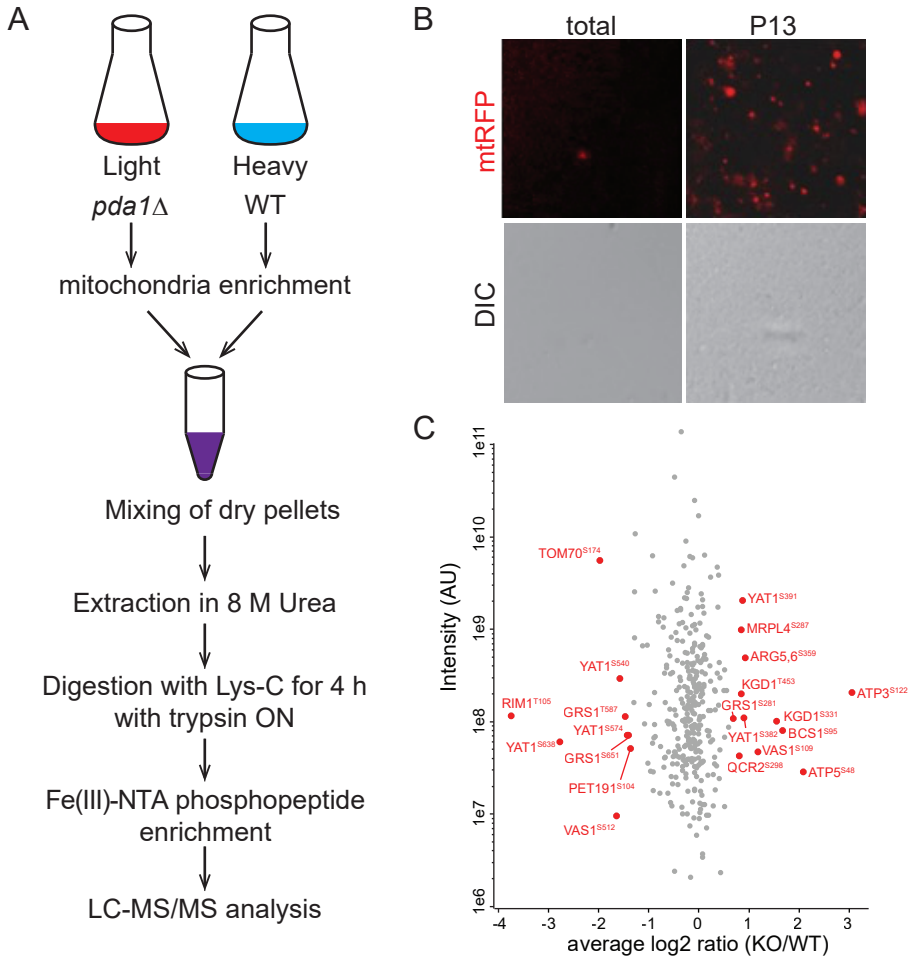
A
Light
pda1Δ
Heavy
WT
mitochondria enrichment
Mixing of dry pellets
Extraction in 8 M Urea
Digestion with Lys-C for 4 h
with trypsin ON
Fe(III)-NTA phosphopeptide
enrichment
LC-MS/MS analysis
B
total
P13
mtRFP
DIC
C
Intensity (AU)
average log2 ratio (KO/WT)
TOM70S174
YAT1S391
MRPL4S287
ARG5,6S359
YAT1S540
KGD1T453
ATP3S122
RIM1T105
GRS1T587
GRS1S281
KGD1S331
YAT1S574
YAT1S382
BCS1S95
YAT1S638
VAS1S109
GRS1S651
QCR2S298
ATP5S48
PET191S104
VAS1S512

Figure 5

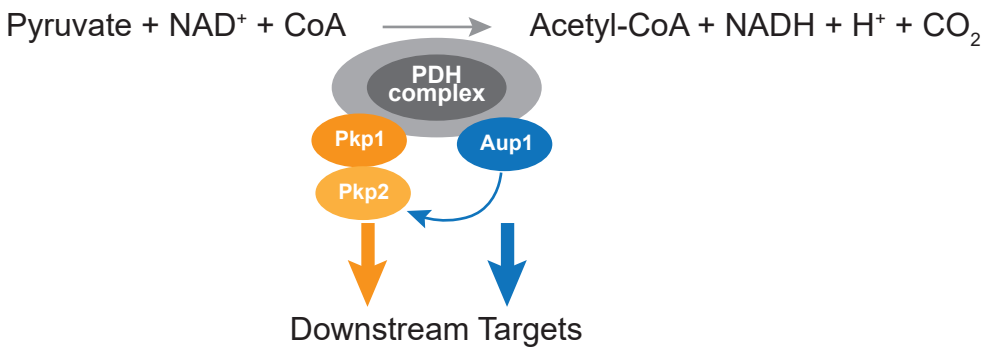
Pyruvate + NAD+ + CoA
Acetyl-CoA + NADH + H+ + CO2
PDH complex
Pkp1
Aup1
Pkp2
Downstream Targets

Figure 6